(41) Ryckaert, J. P.; Ciccotti, G.; Berendsen, H. J.; J. Comput. Phys. 1977, 23, 327.
(42) Ciccotti, G.; Ferrario, M.; Ryckaert, J. P. Mol. Phys. 1982, 47, 1253.
(43) van Gunsteren, W. F.; Karplus, M. Macromolecules 1982, 15, 1528.
(44) Hogan, M.; Wang, J.; Austin, R. H.; Monitto, C. L.; Hershkowitz, S. Proc. Natl. Acad. Sci. U.S.A. 1982, 79, 3518.
(45) Hogan, M.; Le Grange, J.; Austin, R. H. Nature (London) 1983, 304, 752.
(46) Thomas, J. C.; Schurr, J. M. Biochemistry 1983, 22, 6194.
(47) Shore, D.; Baldwin, R. L. J. Mol. Biol. 1983, 170, 957, 983.
(48) Horowitz, D. S.; Wang, J. C. J. Mol. Biol. 1984, 173, 75.
(49) Carpenter, D. K.; Skolnick, J. Macromolecules 1981, 14, 1284.
(50) Harris, R. A.; Hearst, J. E. J. Chem. Phys. 1966, 44, 2595.

Static and Dynamic Properties of Polystyrene in Good Solvents: Ethylbenzene and Tetrahydrofuran

K. Venkataswamy and A. M. Jamieson*

Department of Macromolecular Science, Case Western Reserve University, Cleveland, Ohio 44106

R. G. Petschek

Department of Physics, Case Western Reserve University, Cleveland, Ohio 44106.
Received January 25, 1985

ABSTRACT: We report static and dynamic light scattering studies of polystyrenes of narrow molecular weight distribution in ethylbenzene (EtPh) and tetrahydrofuran (THF) as solvents. These experiments generate values for z-average radius of gyration, $\langle R_g \rangle_z$, weight-average second osmotic virial coefficient, A_2, z-average translational diffusion coefficients, $\langle D_t \rangle_z$, and hence the diffusion virial coefficients, k_D, and the z-average of the inverse frictional radius, $\langle R_f^{-1} \rangle_z$. The results show that while for a specific molecular weight the $\langle R_g \rangle_z$ values in THF are similar to our experimental values in ethylbenzene and to literature values in benzene or toluene, the A_2 values, as well as hydrodynamic radii, are substantially larger for THF. We find that values of "universal ratios" of static and dynamic quantities in ethylbenzene are in good agreement with predictions of renormalization group theory appropriate to the nondraining good-solvent limit, while those for THF are not. We present a more stringent test of universality by plotting the static light scattering data directly in a "scaling" form. Identical polystyrene samples in THF and ethylbenzene are clearly different when analyzed in this way, although they do conform to an empirical universal description for solvents of arbitrary quality. These analyses suggest that in THF polystyrene exists in a more flexible conformation and is closer to the nondraining, good-solvent limit.

Background

Interest in measurements of the transport properties of polymer chains in good solvents has revived recently because of new theoretical developments that have established procedures by which realistic predictions of experimental parameters can be made for such systems. On the one hand, numerical simulations of chain dynamics, usually using Monte Carlo methods previously confined to Gaussian chains,[1,2] can now be extended to self-avoiding walks,[3-5] thus enabling one to incorporate the excluded-volume effect. On the other hand, successful application of renormalization group (RG) techniques[6] to describe features of polymer chain statistics with excluded volume[7,8] have led recently to RG calculations of polymer hydrodynamic parameters.[9-12]

Theory predicts[7,9] and experiment appears to confirm[13,14] that structural radii, R, exhibit power scaling laws against molecular weight, M, of the form

$$R \sim M^{\nu} \tag{1}$$

where ν is a characteristic exponent. For Gaussian coils, $\nu = 0.5$ and, as solvent quality increases, ν rises smoothly to the asymptotic value $\nu = 0.588$. Experiment indicates[13,14] that the crossover occurs more sharply for the static radius $\langle R_g \rangle_z$ than for the hydrodynamic radii. Recent RG calculations further predict specific values for certain universal ratios of static and hydrodynamic parameters.[9] These are

$$\psi = \frac{A_2 M^2}{4\pi^{3/2} N_A \langle R_g^2 \rangle^{3/2}} \tag{2}$$

$$U_{A\eta} = \frac{A_2 M}{[\eta]} \tag{3}$$

$$U_{f\eta} = \frac{f}{\langle R_g^2 \rangle^{1/2} \eta_s} \tag{4}$$

$$U_{\eta\eta} = \frac{M[\eta]}{N_A \langle R_g^2 \rangle^{3/2}} \tag{5}$$

and

$$U_{\eta f} = \left(\frac{M[\eta]}{N_A} \right)^{1/3} \frac{\eta_s}{f} \tag{6}$$

where the frictional coefficient $f = 6\pi\eta_s R_f = kT/6\pi\eta_s D^0_t$ and D^0_t is the limiting translational diffusion coefficient. In eq 2-6, $[\eta]$ is the intrinsic viscosity, η_s is the solvent viscosity, N_A is Avogadro's number, k is the Boltzmann constant, and T is absolute temperature. These quantities have been calculated recently[9] for both the Θ and asymptotic good-solvent limit, the hydrodynamics being formulated within the Kirkwood-Riseman model with a full Oseen tensor description.

Polystyrene is one of the most widely studied polymers because of the availability of polymer samples of narrow

0024-9297/86/2219-0124$01.50/0

molecular weight distribution. A substantial amount of work covering a wide range of molecular weights has already been reported in the literature for "good" solvents such as benzene,[15-17] toluene,[18-20] and tetrahydrofuran (THF).[20-24] In this paper we report results of photon correlation spectroscopy and viscosity experiments on polystyrene in ethylbenzene (EtPh) and THF. The experimental quantities of interest are the translational diffusion coefficient, $\langle D_t \rangle_z$, the intrinsic viscosity $[\eta]$, the z-average radius of gyration, $\langle R_g \rangle_z$, and the second virial coefficients A_2. Our static and dynamic light scattering results on a wide range of molecular weights (0.1×10^6–8.5×10^6) in ethylbenzene are the first reported for this solvent. We compare these results with the chemically similar solvents toluene and benzene. In THF, we have extended the experimental information[24] on $\langle R_g \rangle_z$ and A_2 to higher molecular weights.

Experimental Section

Materials. Polystyrene standards of very narrow molecular weight distribution were purchased from Pressure Chemicals and Toya Soda (Japan). The weight-average molecular weights ranged from 0.1×10^6 to 8.48×10^6. The sample was used as purchased and was not further purified. THF (reagent grade) and EtPh (spectroscopic grade) were obtained from Aldrich Chemical Co. The physical constants of THF at 30 °C were refractive index $n_{30°C} = 1.403$, viscosity $\eta = 0.438$ cP, and with polystyrene solute $(dn/dc)_{30°C} = 0.2133$ mL/g. For ethylbenzene at 25 °C the physical constants were refractive index $n_{25°C} = 1.495$, viscosity $\eta = 0.619$ cP, and with polystyrene $(dn/dc)_{25°C} = 0.106$ mL/g. Since recent work has noted[25] that THF is hygroscopic and that the presence of significant amounts of water can markedly alter the thermodynamic properties of solutions of polystyrene in THF, we felt it necessary to determine the water content of our THF solvent. Using the Karl Fischer titration assay (photovolt Aquatest IV), we found our THF contained 0.09% H_2O. This level of water should have negligible impact on the solution thermodynamics.[25]

Solutions were prepared by dissolving a known quantity of the polymer in the solvent, which was filtered thoroughly prior to use. Filtrations were carried through 0.2-μm and 0.5-μm Millipore Teflon filters under the influence of gravity. This was done to avoid any shear degradation of the polymer during filtration, and our light scattering measurements corroborated this fact. Filtrations were repeated until the samples were free from dust particles, which are centers for parasitic scattering.

For light scattering measurements, the samples were diluted into sealed scattering cells and further centrifuged at low speeds, 5000 rpm for 30 min to 1 h prior to experimentation. Fortunately, because of the ease of dissolution of polystyrene in THF and EtPh, it was possible to carry out a complete light scattering analysis on freshly prepared solutions, i.e., within a 12-h period after dissolution.

Methods. Two instruments were employed to carry out the static and dynamic light scattering experiments: a custom-built system, which has been described elsewhere,[26] utilizing a Coherent Radiation Model 42 Ar^+ laser ($\lambda = 4880$ Å) with a Saicor 42 digital correlator and an Ortec photon counter to measure the mean value of the intensity of the scattered light, and a Brookhaven Instrument Corp. spectrometer comprising a BI 2000 goniometer and BI 2020 correlator with Spectra Physics 15-mW He/Ne laser ($\lambda = 6328$ Å). The temperature of measurements was 298 K for PS in EtPh and 303 K for PS in THF, in each case controlled to within ±0.1 K.

The weight-average molecular weight M_w, second virial coefficients A_2, and z-average radius of gyration $\langle R_g \rangle_z$ were obtained by measuring the average intensity of the scattered light as a function of angle and concentrations. For low molecular weights, the extrapolations were carried out at a finite angle ($\theta = 40°$). The working equation for the excess Rayleigh's ratio R_θ is given by

$$\frac{Kc}{\Delta R_\theta} = \frac{1}{M_w P(\theta)} + 2A_2 c + 3A_3 c^2 + \dots \tag{7}$$

where K is the optical constant of the system and A_2 and A_3 are the second and third osmotic virial coefficients, respectively. $P(\theta)$, the particle scattering function, can be expressed in terms of the solvent refractive index n and wavelength of incident light λ in vacuo as

$$P^{-1}(\theta) = \left\{1 + \frac{16\pi^2 n^2 \langle R_g^2 \rangle_z}{3\lambda^2} \sin^2(\theta/2) + \dots\right\} \tag{8}$$

For low molecular weights ($M_w \leq 0.6 \times 10^6$), $P(\theta) = 1$ within experimental error at accessible angles and eq 7 reduces to

$$\frac{Kc}{\Delta R_\theta} = \frac{1}{M_w} + 2A_2 c + 3A_3 c^2 + \dots \tag{9}$$

The high molecular weight samples exhibited curvature in Zimm plots,[27] and hence square-root plots[28] were employed. Taking square roots of eq 7 and substituting $A_3 = (1/3)A_2 M_w$, one can write

$$(Kc/\Delta R_\theta)^{1/2}{}_{\theta \to 0} = (1/M_w^{1/2})(1 + A_2 M_w c) \tag{10a}$$

and

$$(Kc/\Delta R_\theta)^{1/2}{}_{c \to 0} = \frac{1}{M_w^{1/2}}\left(1 + \frac{8\pi^2 n^2}{3\lambda^2}\langle R_g^2 \rangle_z \sin^2\frac{\theta}{2}\right) \tag{10b}$$

In our calculation, higher order virial coefficeints ($>A_3$) are assumed equal to 0. A_2 is evaluated from the slope of $(Kc/\Delta R_\theta)^{1/2}{}_{\theta \to 0}$ against concentration, whereas $\langle R_g^2 \rangle^{1/2}{}_z$ was obtained by the slope of $(Kc/\Delta R_\theta)^{1/2}{}_{c \to 0}$ against $\sin^2(\theta/2)$. Our experiments were carried out in the angular range of 30–65° at intervals of 5°. For the lowest molecular weight for which $\langle R_g \rangle_z$ is reported here ($M_w = 0.9 \times 10^6$), measurements were carried out over a much wider angular range (30–145°). Measurements below 30° were not reproducible due to scattering from the cell walls. The molecular weights obtained by the extrapolation of $(Kc/\Delta R_\theta)^{1/2}{}_{c \to 0}$ to 0 angle and $(Kc/\Delta R_\theta)^{1/2}{}_{\theta \to 0}$ to 0 concentration were equal within the experimental error (<1%), and average values are reported here. The intensity measurements were repeated and are reproducible to within a few percent.

The z-average translational diffusion coefficients $\langle D_t \rangle_z$ were determined by moment analysis of the correlation function given by[26]

$$C(\tau) = \int_0^\infty G(\Gamma) \exp(-\tau\Gamma)\, d\Gamma \tag{11}$$

where $\bar{\Gamma} = \int_0^\infty G(\Gamma)\Gamma\, d\Gamma$ is the mean relaxation rate. Expansion of the correlation function as a Taylor series

$$\ln C(\tau) = -\bar{\Gamma}\tau + \frac{1}{2!}\frac{\mu_2}{\bar{\Gamma}^2}(\bar{\Gamma}\tau)^2 + \dots \tag{12}$$

where the first moment, $\bar{\Gamma}$, can be related to the z-average translational diffusion coefficient $\langle D_t \rangle_z$ by

$$\bar{\Gamma} = 2\langle D_t \rangle_z q^2 \tag{13}$$

where $q = (4\pi n/\lambda) \sin(\theta/2)$, λ is the wavelength of the light in vacuum, n is the refractive index of the medium, and θ is the scattering angle. The second moment, μ_2, is the variance in Γ:

$$\mu_2 = \langle \Gamma^2 \rangle - \bar{\Gamma}^2 \tag{14}$$

A typical correlation function is shown in Figure 1. The first and second moments were determined by moment analysis described above. For molecular weights less than 1.0×10^6, the experiments were carried out at a single angle $\theta = 40°$ ($qR_g \ll 1$), and the second moment μ_2 was small (<0.06) owing to the low M_w/M_n values. For molecular weights greater than 1.8×10^6, the angular dependence of the translational diffusion coefficient was measured. The translational diffusion coefficient at a finite concentration, c, was determined by linear extrapolation of the data at a finite q vector to 0 angle according to the relationship[29]

$$\langle D_t \rangle_q = \langle D_t \rangle_z (1 + \chi^2 q^2) \tag{15}$$

where χ is a constant of proportionality and then to 0 concentration to evaluate $\langle D^0_t \rangle_z$.

Viscosity measurements for polystyrene in ethylbenzene were carried out by using Ubbelohde viscometers, and the flow times

Table I
Results of Static Light Scattering of Polystyrene by Berry Plots

		ethylbenzene			in THF		
$M_w \times 10^{-6}$ [a]	M_w/M_n	M_w	$\langle R_g\rangle_z \pm 5\%$, Å	$A_2 \times 10^{-3} \pm 8\%$, cm³·mol/g²	M_w	$\langle R_g\rangle_z \pm 5\%$, Å	$A_2 \times 10^{-3} \pm 8\%$, cm³·mmol/g²
0.1[b]	1.06	0.093					
0.3[b]	1.06	0.307		0.358			
0.6[b]	1.10	0.620		0.310			
0.9[b]	1.10	0.895	435	0.248	0.890	438	0.3956
1.80[b,c]	1.30	1.85	620	0.210	1.82	590	0.2945
3.84[c]	1.04	3.88	950	0.170	3.71	945	0.257
5.48[c]	1.15	5.63	1182	0.161	5.55	1180	0.22
8.46[c]	1.17	8.46	1608	0.140	8.42[d]	1372[d]	0.2063

[a] Suppliers specifications, c. Experimental values corrected by $\langle R_g\rangle_w = \langle R_g\rangle_z[(1 \pm U)/(1 + 2U)^{1/2}]$, where $U = M_w/M_n - 1$. [b] Samples from Pressure Chemicals. [c] From Toya Soda. [d] Fujita plot.[19]

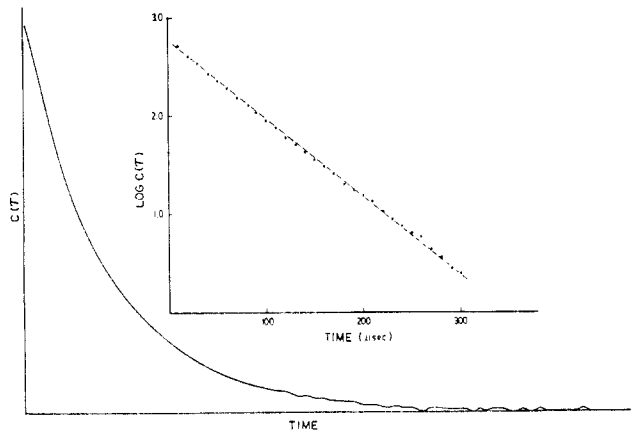

Figure 1. Typical photon correlation function of polystyrene in ethylbenzene ($M_w = 0.9 \times 10^6$, sample time = 10 μs) at 40° scattering angle. The insert shows the first 30 points used in analysis by the method of cumulants.

were chosen such that the kinetic energy corrections were negligible. The intrinsic viscosity was determined by extrapolating reduced specific viscosity as well as $[(\ln \eta_r)/c] - 1$ to 0 concentration according to Huggins and Kraemer's equations, respectively (eq 16 and 17)

$$\eta_{sp}/c = [\eta] + K_1[\eta]^2c + \ldots \quad (16)$$

$$[(\ln \eta_r)/c] - 1 = [\eta] - K_1'[\eta]c + \ldots \quad (17)$$

Results

Excess Intensity Measurements. Excess intensity data for PS in EtPh, measured as a function of scattering angle and concentration and analyzed by square-root plots, are shown in Figure 2. The weight-average molecular weight M_w was determined by the intercept, and A_2 and $\langle R_g\rangle_z$ were determined by slopes of $(c/\Delta R_\theta)^{1/2}{}_{\theta\to 0}$ against c (Figure 2a) and $(c/\Delta R_\theta)^{1/2}{}_{c\to 0}$ against $\sin^2(\theta/2)$ (Figure 2b), respectively (as per eq 10). For THF, square-root plots of data extrapolated respectively to the limits of zero angle and concentration for various molecular weights are shown in parts a and b of Figure 3. We could not employ Zimm plots for these systems, as they exhibited curvature as observed in other good solvents.[15,17,19] Our angular intensity measurements are limited to scattering angles above 30°. However, we note that our angular extrapolations lead to accurate molecular weight measurements and are similar to literature data for polystyrenes in benzene and toluene. We thus believe that our $\langle R_g\rangle_z$ values are accurate in the molecular weight range studied (0.9×10^6–8.48×10^6). The results of the excess light scattering measurements are listed in Table I. Our M_w values, measured in two different solvents, are within experimental error, in good agreement with the supplier's specifications. The results for radii of gyration $\langle R_g\rangle_z$ are comparable numerically to values reported in other good solvents.[15,17,18,23] The A_2 values for polystyrene in EtPh are similar to reported values for toluene.[19]

Figures 4 and 5 display the logarithmic plots of radius of gyration $\langle R_g\rangle_z$ and second virial coefficients, respectively, for PS in THF and EtPh. In the molecular weight range studied, the plots are linear and can be best represented by the following least-square fits:

in ethylbenzene

$$\langle R_g^2\rangle^{1/2}{}_z = (0.1725 \pm 0.004)M_w^{0.57\pm0.01}\ (\text{Å}) \quad (18)$$

$$A_2 = (0.011 \pm 0.005)M_w^{-0.27\pm0.02}\ \text{cm}^3\cdot\text{mol/g}^2 \quad (19)$$

in THF

$$\langle R_g^2\rangle^{1/2}{}_z = (0.2092 \pm 0.01)M_w^{0.56\pm0.02}\ (\text{Å}) \quad (20)$$

$$A_2 = (0.0194 \pm 0.004)M_w^{-0.286\pm0.02}\ \text{cm}^3\cdot\text{mol/g}^2 \quad (21)$$

Our experimental $\langle R_g\rangle_z$ values for PS in THF are in good agreement with the earlier study of Baumann,[24] and our A_2 values are consistent with two earlier sources.[29,30] Within experimental error, the literature values of $\langle R_g\rangle_z$ for PS in toluene and benzene are in agreement with our results. When experimental values of second virial coefficients A_2 are compared with literature, there are clearly systematic differences between PS in THF against PS in benzene, toluene, or ethylbenzene.

Dynamic Light Scattering. Figure 6 exhibits the concentration dependence of translational diffusion coefficients for PS in EtPh. For high molecular weight samples ($>1.8 \times 10^6$), the translational diffusion at a finite concentration was evaluated by extrapolating experimental values of Γ to 0 angle (eq 15). The concentration dependence of the translational diffusion can be expressed as

$$\langle D_t\rangle_z = \langle D^0{}_t\rangle_z(1 + k_Dc) \quad (22)$$

where $\langle D^0{}_t\rangle_z$ is the value at infinite dilution. k_D represents the concentration dependence and can be evaluated by

$$k_D = (1/\langle D^0{}_t\rangle_z)\left(\frac{d\langle D_t\rangle_z}{dc}\right)_T \quad (23)$$

The limiting value of the translational diffusion coefficient can be written in terms of its hydrodynamic radius R_f by the Stokes–Einstein equation:[31]

$$\langle D^0{}_t\rangle_z = kT/6\pi\eta_sR_f \quad (24)$$

The experimental values $\langle D^0{}_t\rangle_z$, R_f, k_D, and M_w are shown in Table II. The translational diffusion coefficients measured in this work for PS in EtPh differ from results reported in an earlier study.[32] However, the latter represent weight-average values by sedimentation–diffusion

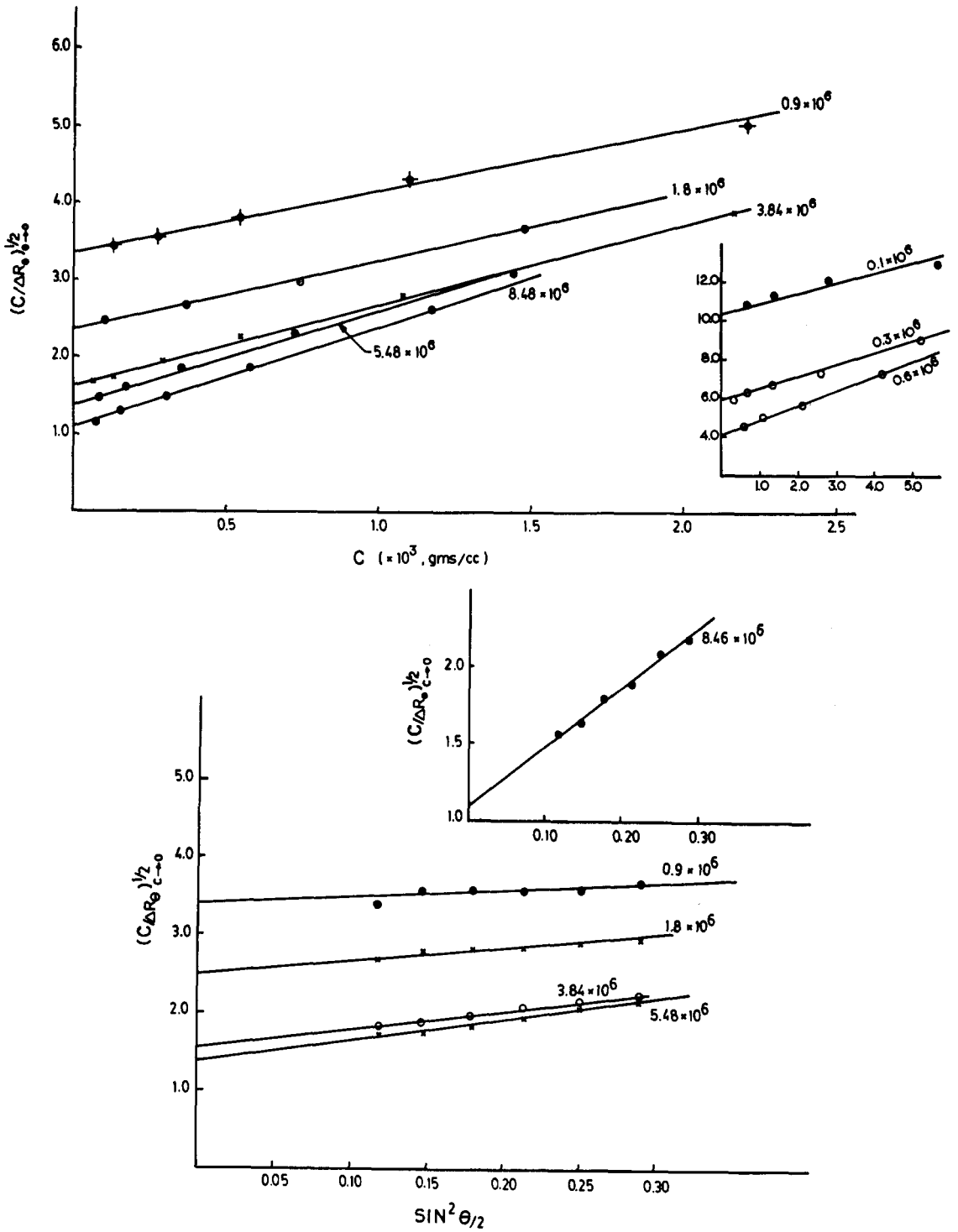

Figure 2. (a) Berry plot of PS in EtPh for the molecular weight range of 0.1×10^6–8.48×10^6. $(c/\Delta R_\theta)^{1/2}$ as a function of concentration extrapolated to 0 angle. (b) $(c/\Delta R_\theta)^{1/2}$ as a function of scattering angle extrapolated to 0 concentration (for $M_w = 0.9 \times 10^6$–8.48×10^6).

experiments on relatively polydisperse samples. In Figure 7 we plot the $\langle D^0_t \rangle_z$ values as a function of molecular weight and determine the scaling relationship

$$\langle D^0_t \rangle_z = (2.88 \pm 0.04 \times 10^{-4}) M_w^{0.56 \pm 0.01} \text{ cm}^2/\text{s} \quad (25)$$

The exponent, $\gamma = 0.56$ in eq 25 is comparable to values reported for polystyrenes in benzene,[16] toluene,[18] and THF.[21]

We have previously reported extensive measurements of $\langle D^0_t \rangle_z$ for polystyrenes in THF.[33] Several additional measurements were made in this study. In Figure 8, we present results of a dual extrapolation to 0 concentration and 0 angle of the $\langle D_t \rangle_z^{app}$ values for a polystyrene of M_w

Table II
Dynamic Light Scattering Results of Polystyrene in Ethylbenzene at 25 °C

$M_w \times 10^{-6}$	$\langle D^0_t \rangle_z \times 10^{-7}$, cm²/s	R_f, Å[a]	k_D(exptl), cm³/g	$k_D(y)$,[b] cm³/g
0.1	4.54	78	23.23	11.97
0.3	2.40	147	38.65	59.20
0.6	1.64	215	164.22	107.01
0.9	1.36	260	187.60	129.29
1.8	0.88	401	243.30	212.022
3.84	0.63	560	368.90	406.86
5.48	0.45	784	401.90	483.97

[a] Calculated by the Stokes–Einstein equation (eq 16). [b] $k_D(y) = 0.8A_2M - (A_A V_h/M) - \bar{\nu}$.

Table III
Dynamic Parameters of Polystyrene in Tetrahydrofuran (30 °C)

$M_w \times 10^6$	$\langle D^0_t \rangle_z \times 10^7$	R_f, Å	$[\eta]^a$	R_η, Å^a	$k_D \times 10^{-2}$, cm^3/g	$k_D(y) \times 10^{-2}$, cm^3/g
0.037	8.81	57.5	23.87	52.7	0.24	0.136
0.051	8.02	63.15	29.98	63.3	0.14	0.170
0.110	4.92	102.94	51.75	98.1	0.32	0.34
0.180	3.25	155.03	73.40	130.0	0.36	0.22
0.39	2.48	204.20	127.10	202	0.96	0.75
0.411	2.51	201.78	131.92	208	0.75	0.98
0.60	1.93	262.41	172.58	259	0.98	1.04
1.80^b	1.05	482.34	376.50	489	2.39	2.794
3.00	0.813	622.95	541.10	649	3.9	3.90
5.48^b	0.585	865.75	829.90	930	15.62	6.716
7.6	0.435	1164.27	1046.82	1104	6.20	10.3

^{a} Values calculated from $[\eta] = 1.363 \times 10^{-2} M_w^{0.71}$ cm^3/g at 25 °C.[18] ^{b} Current experimental values.

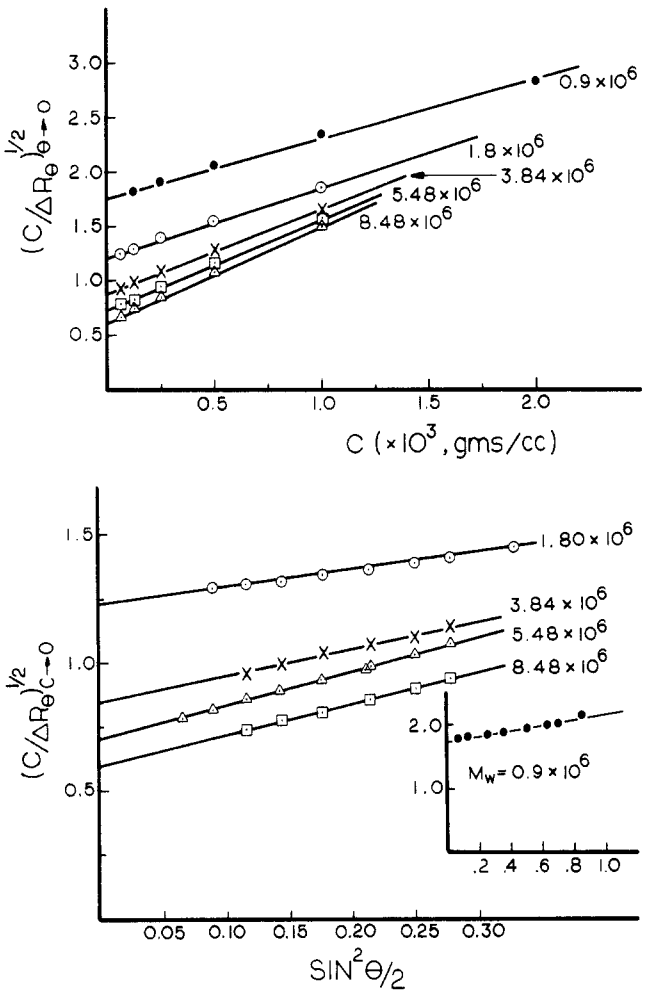

Figure 3. (a) Berry plot of PS in THF for the molecular weight range of 0.9 × 10^6–8.48 × 10^6. $(c/\Delta R_\theta)^{1/2}$ as a function of concentration extrapolated to 0 angle. (b) $(c/\Delta R_\theta)^{1/2}$ as a function of scattering angle extrapolated to 0 concentration (for M_w = 0.9 × 10^6–8.48 × 10^6).

= 5.48 × 10^6 in THF at 30 °C from which we determine $\langle D^0_t \rangle_z = 5.85 \times 10^{-8}$ cm^2/s. When η_s = 0.438 cP is used, this corresponds to a hydrodynamic radius R_f = 870 Å. Also in Figure 8, we show a similar extrapolation for the same polystyrene sample in ethylbenzene from which we deduce $\langle D^0_t \rangle_z = 4.50 \times 10^{-8}$ cm^2/s and, with η_s = 0.619 cP, R_f = 780 Å. Our recent experiments are consistent with our earlier conclusion[17,18] that for polystyrene in THF at 30 °C

$$\langle D^0_t \rangle_z = 3.4 \times 10^{-4} M_w^{-0.56} \text{ cm}^2/\text{s} \quad (26)$$

Also, we find that R_f values for polystyrene in THF are

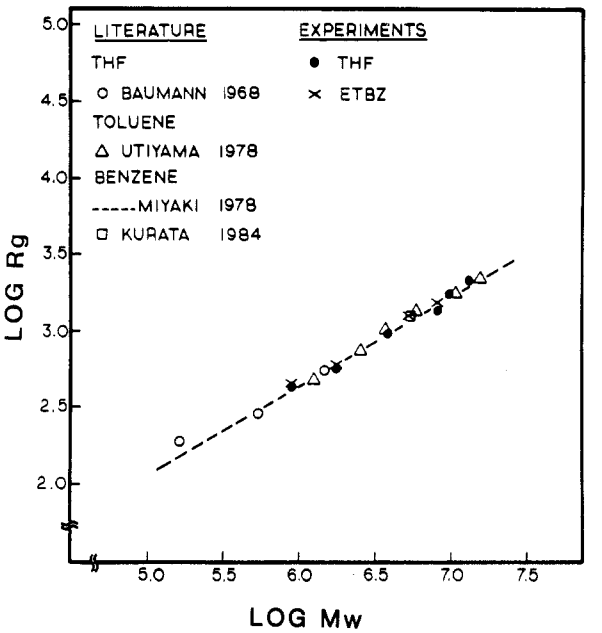

Figure 4. Logarithmic plot of z-average radius of gyration $\langle R_g \rangle_z$ against molecular weight.

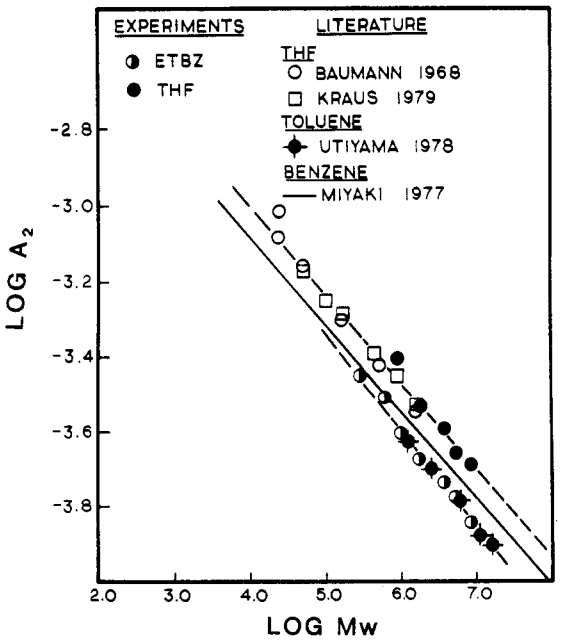

Figure 5. Logarithmic plot of second virial coefficient against molecular weight.

uniformly larger than in ethylbenzene (or in benzene[16] or toluene[19]). In Table III we list $\langle D^0_t \rangle_z$ and R_f values de-

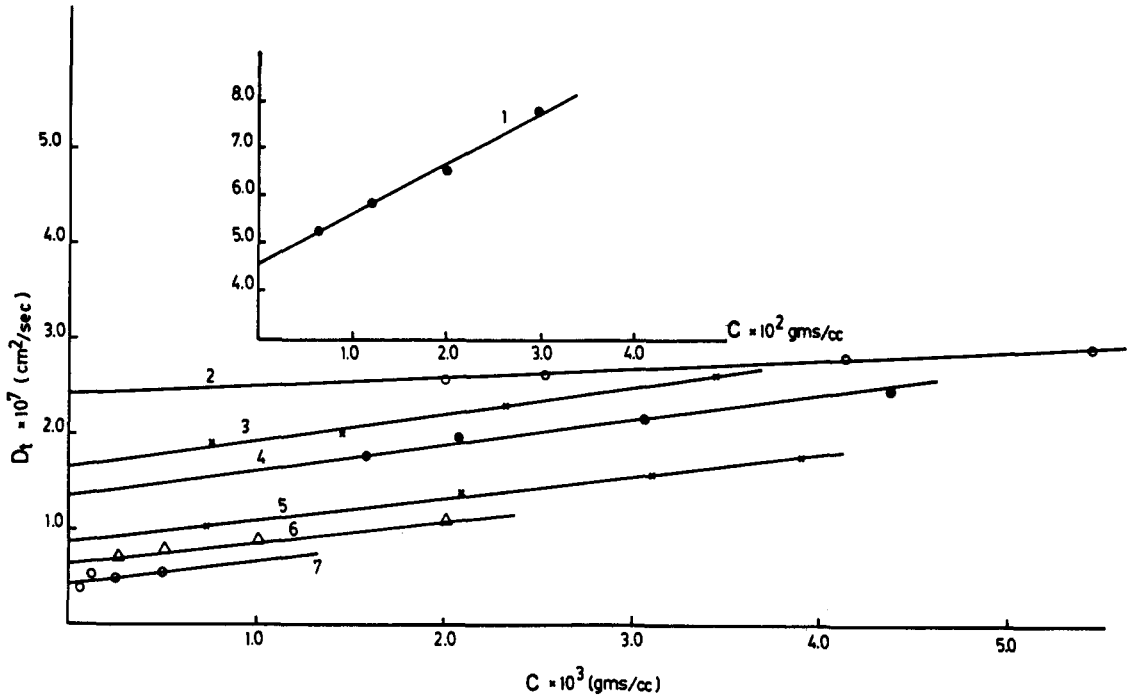

Figure 6. Translational diffusion coefficients as a function of concentration: (1) 0.1×10^6; (2) 0.3×10^6; (3) 0.6×10^6; (4) 0.9×10^6; (5) 1.8×10^6; (6) 3.84×10^6; (7) 5.48×10^6.

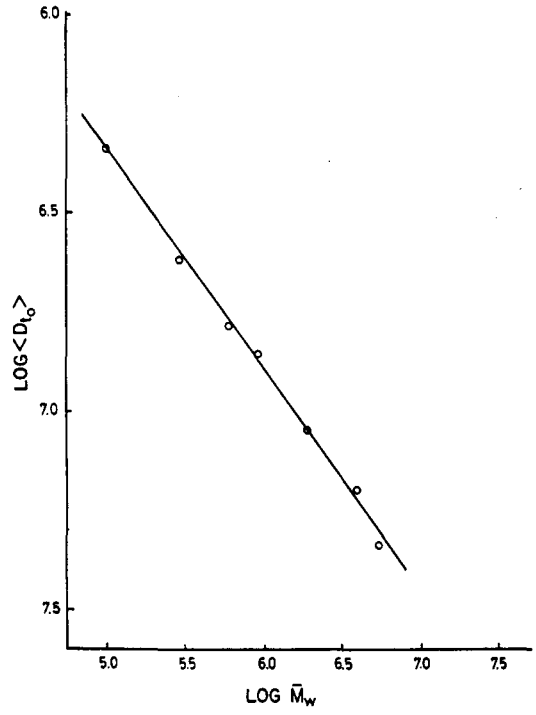

Figure 7. Log $\langle D^0_t \rangle_z$ against molecular weight.

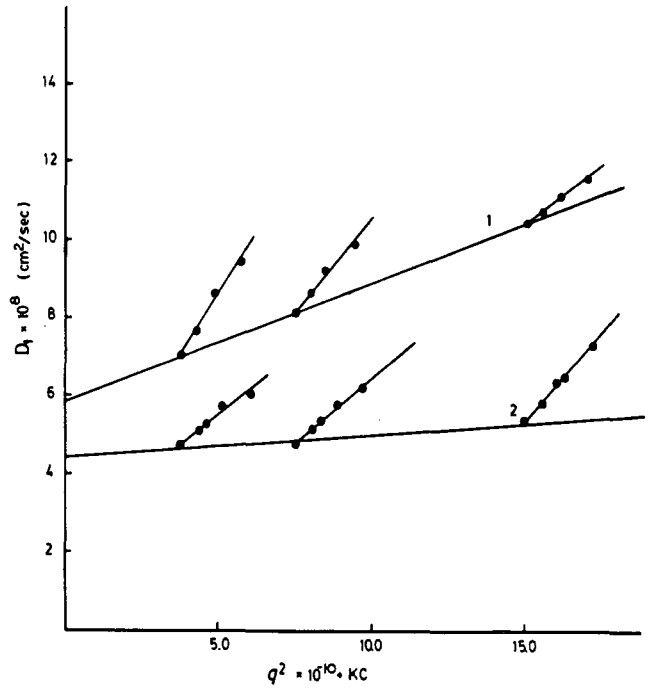

Figure 8. Translational diffusion coefficient D_t as a function of q vector and concentration for Toya Soda polystyrene of $M_w = 5.48 \times 10^6$: (1) THF at 30 °C; (2) ethylbenzene at 25 °C.

termined in our previous work. Also, we present the values of k_D, the concentration dependence of the translational diffusion coefficients. The k_D values are compared with the theoretical predictions of Yamakawa[34] in Tables I and III:

$$k_D(y) = 0.8A_2M - (N_A V_h/M) - \bar{v} \quad (27)$$

It is relevant to note that our R_f data in THF are very consistent with an independent study[35] for the same system at 25 °C.

Intrinsic Viscosity. In Figure 9, we plot the relative viscosity data for polystyrene in ethylbenzene according to eq 16 to determine the intrinsic viscosity. The intrinsic viscosity is related to molecular weight (Figure 10) by the following Mark–Houwink relationship. The intrinsic viscosity is comparable with the literature values.[36]

$$[\eta] = (0.0142 \pm 0.001)M_w^{0.70\pm0.02}\ \text{cm}^3/\text{g} \quad (28)$$

Intrinsic viscosity can be expressed in terms of an equivalent hard-sphere radius R_η by Einstein's relationship

$$[\eta] = 2.5N_A V_h/M \quad (29)$$

where N_A is Avogadro's number and $V_h = 4/3\pi R_\eta^3$. The experimental values $[\eta]$, K_1, K_1', and R_η are displayed in Table IV. We list in Table III $[\eta]$ values (and corresponding hydrodynamic radii, R_η) calculated from the experimental relation generated by Appelt and Meyerhoff[18,23] from extensive experiments carried out on a very

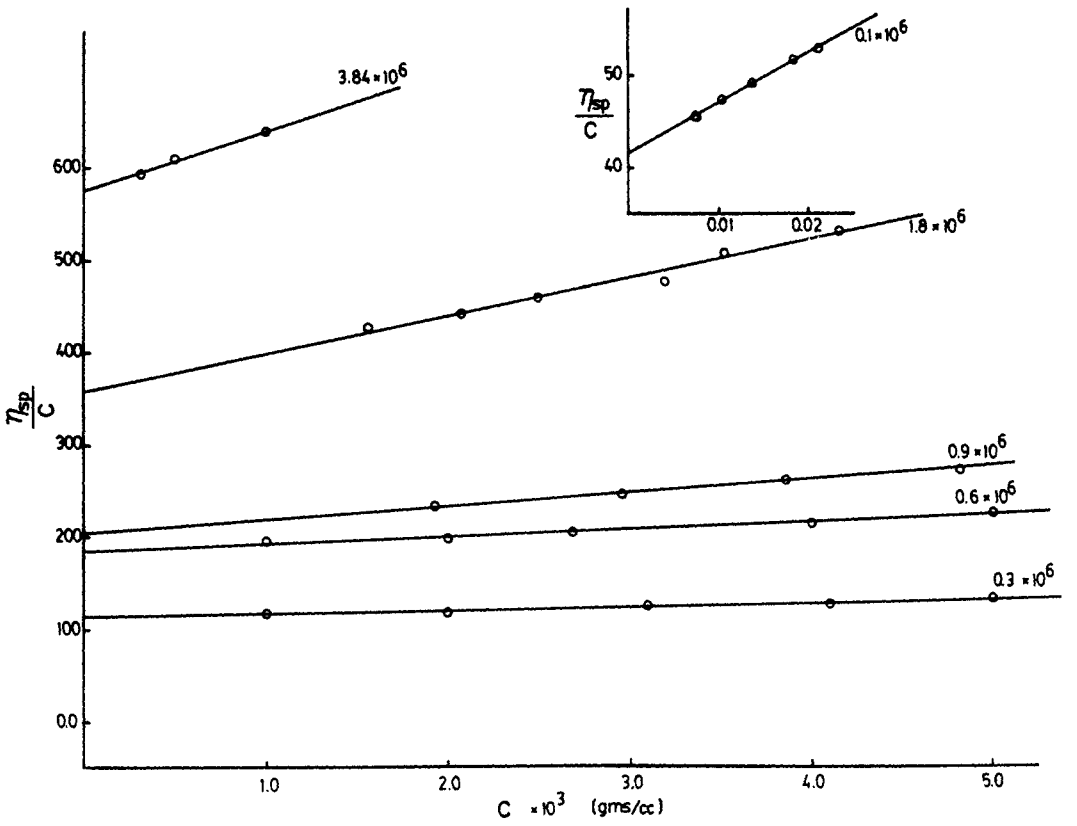

Figure 9. η_{sp}/c plotted against concentration. The insert is the data for $M_w = 0.1 \times 10^6$. The data for 3.84×10^6 are corrected for shear rate dependence.

Table IV
Experimental Values of Intrinsic Viscosity as a Function of Molecular Weight for Polystyrene in Ethylbenzene

$M_w \times 10^{-6}$	$[\eta]$, cm^3/g	k_1	k_1'	R_η, Å[a]
0.1	41.5	0.3029	0.215	85.0
0.3	114			177.0
0.6	183	0.256	0.191	262.0
0.9	206	0.343	0.157	308.0
1.8	355	0.33	0.15	466.0
3.84	575[b]	0.203	0.22	707.0

[a] Calculated by Einstein's formula for intrinsic viscosity (eq 19). [b] Values estimated as the mean of the Huggins and Kraemer extrapolations.

wide range of molecular weights in THF [$0.2 \times 10^6 < M_w < 4 \times 10^7$]:

$$[\eta] = 1.363 \times 10^{-2} M_w^{0.71} \quad (30)$$

Discussion

We begin by noting that the equilibrium properties $\langle R_g \rangle_z$ and A_2 for polystyrene in ethylbenzene are reported here for the first time. Also, this study is the first for polystyrene in ethylbenzene by dynamic light scattering experiments. $\langle R_g \rangle_z$ data are numerically comparable with values reported for polystyrene in known good solvents,[15,17,18,24] indicating that ethylbenzene has similar solvating power to toluene and benzene as well as THF. The hydrodynamic radii R_f and R_η are also similar to values reported in toluene[18] and benzene.[16] It is not surprising that the static and dynamic properties of polystyrene are similar in the three aromatic solvents in view of the similarities in chemical structure.

Our results indicate, somewhat surprisingly since THF is a polar solvent, that although within experimental error, $\langle R_g \rangle_z$ values in THF are equivalent to those in ethylbenzene, as seen in Table I and Figure 4, the A_2 values are much larger in THF (Table I and Figure 5). Also, the hydrodynamic radii, R_f and R_η, are larger in THF than in ethylbenzene, as can be seen by comparing Tables II and IV with Table III. Figure 5 indicates that A_2 values delineate small differences in solvent power more clearly than the $\langle R_g \rangle_z$ values, in qualitative agreement with theoretical expectation. Clearly from Figure 5, THF is a better solvent for polystyrene. In order to rationalize the $\langle R_g \rangle_z$, R_f, and R_η data, it is necessary, as discussed below, to postulate that in THF polystyrene undergoes a transition to a more

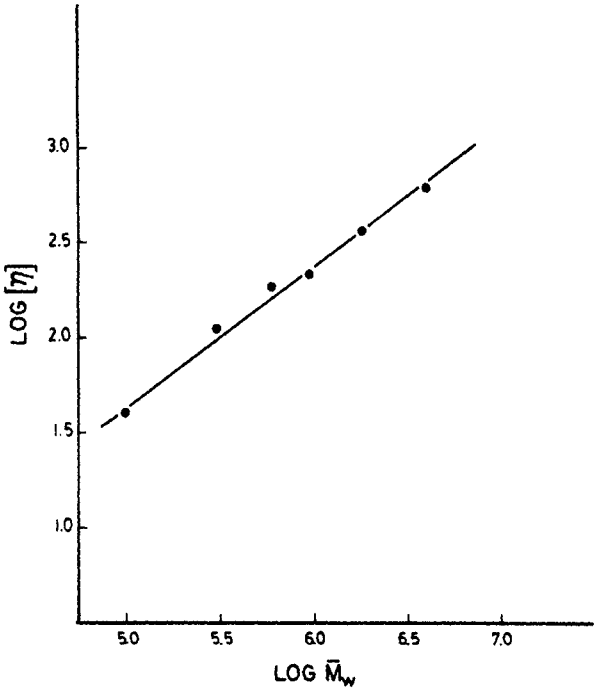

Figure 10. Log $[\eta]$ against log M_w.

Table V
Universal Ratios for Polystyrene in Ethylbenzene and Tetrahydrofuran

$M_w \times 10^{-6}$	ρ_1		ρ_2		ψ		$U_{A\eta}$		U_{fs}		$U_{\eta s}$		$U_{\eta f}$	
	EtPh	THF	EtPh	THF	EtPh	THF	EtPh	THF	EtPh	THF	EtPh	THF	EtPh	THF
0.1	(1.52)[a]	(1.244)	1.09	0.9738			1.14		(12.42)				0.1265	0.1162
0.3	(1.52)	(1.241)	1.20	0.985			0.94		(12.42)				0.1392	0.1183
0.6	(1.57)	(1.241)	1.22	0.992			1.02		(11.99)				0.1416	0.1193
0.9	1.67	1.36	1.28	0.995	0.246	0.2845	1.08	1.547	11.27	13.82	4.91	4.092	0.1375	0.1198
1.8[b]	1.55	1.223	1.16	0.986	0.213	0.348	1.07	1.407	12.19	14.95	4.43	5.506	0.1346	0.1197
3.84	1.70	1.27	1.26	1.01	0.192	0.342	1.16	1.530	11.11	14.92	3.95	5.077	(0.1392)	0.1137
5,48[b]	1.515	1.32		1.035	0.226	0.2982		1.452	(12.43)	13.74	3.662	4.596		0.1209
8.46		1.205		1.018	0.179	0.426		1.54	11.85	(15.52)	3.045	6.1435		0.1203
av	1.61 ± 0.078	1.35 ± 0.06	1.205 ± 0.05	1.00 ± 0.02	0.212 ± 0.023	0.318 ± 0.027	1.07 ± 0.08	1.496 ± 0.05	11.35 ± 0,52	14.42 ± 0.0 58	3.99 ± 0.64	5.083 ± 0.71	0.1318 ± 0.005	0.121 ± 0.01
theory[c]		1.562		1.117		0.219		1.196		12.067		4.078		0.1297

[a] Values in parentheses calculated by Domb–Barret equation. [b] RG theory predictions for a nondraining good-solvent limit.[9] [c] Current experimental values for THF. The values listed for other molecular weights are calculated by $\langle D^3_t \rangle_z = 3.4 \times 10^{-4} M^{-0.56}$ cm²/s.

flexible local conformation which is more swollen and less permeable to the solvent than in ethylbenzene (and hence in benzene and toluene).

We illustrate this situation further by comparing in Table V data for the universal ratios (eq 2–6) of polystyrene in THF and in ethylbenzene. We also list in Table V values for the radius ratios $\rho_1 = \langle R_g \rangle_z / R_f$ and $\rho_2 = R_\eta / R_f$ which are proportional respectively to U_{fs} and $U_{\eta s}$. Table V shows that the experimental values for the various ratios for polystyrene in THF are not in good agreement with the predictions of the RG theory[9] in the nondraining, good-solvent limit, while those in ethylbenzene agree very well. It is, however, very interesting to note that our values in THF for ratios involving hydrodynamic quantities, U_{fs} and $U_{\eta s}$, are consistent with the Monte Carlo predictions by Zimm for a nondraining Gaussian coil. A recent RG calculation[12] predicts, in disagreement with ref 9, that these quantities will in fact be essentially invariant to changes in the excluded-volume interaction, provided the degree of solvent draining remains unchanged. It is, likewise, relevant that as we noted elsewhere,[37] application of porous-sphere hydrodynamic theory[38,39] to our results for the hydrodynamic ratio $U_{\eta f}$ indicates that in THF polystyrene is approximately 3 times less permeable than in ethylbenzene.

The larger values of the quantities $U_{A\eta}$ and ψ for THF reflect the larger values of A_2 as measured from square-root plots. It is noted that the latter are prone to comparatively large experimental errors (±7%) and may also reflect unspecified contributions from higher order virial terms. To exhibit the difference between THF and ethylbenzene more directly, it is instructive to plot the absolute intensity data $\Delta i(q,c)$ in a "scaling" form, viz. $cM_w[\Delta i(q,c)]^{-1}$ vs. $q^2 + kc^{2/3}$ where k is an arbitrary constant. This plot is designed to test the scaling properties in (q, c) space of the universal scaling form factor $F(q,c)$ related to the experimental static structure factor $S(q,c)$ by

$$S(q,c) = cM_w F(q,c) \tag{31}$$

This is done in Figure 11 for the polystyrene having $M_w = 3.84 \times 10^6$. The intensity data for this polymer in THF increase with concentration more rapidly than in ethylbenzene. If a conformational change in polystyrene were solely responsible for the differences seen in THF vs. EtPh, it would be possible to superpose the intensity data in Figure 11 by a change in horizontal length scale. Clearly, this cannot be accomplished with these results. Thus we infer that in THF polystyrene is closer to the good-solvent limit, but, in view of the similarity of R_g values, it appears

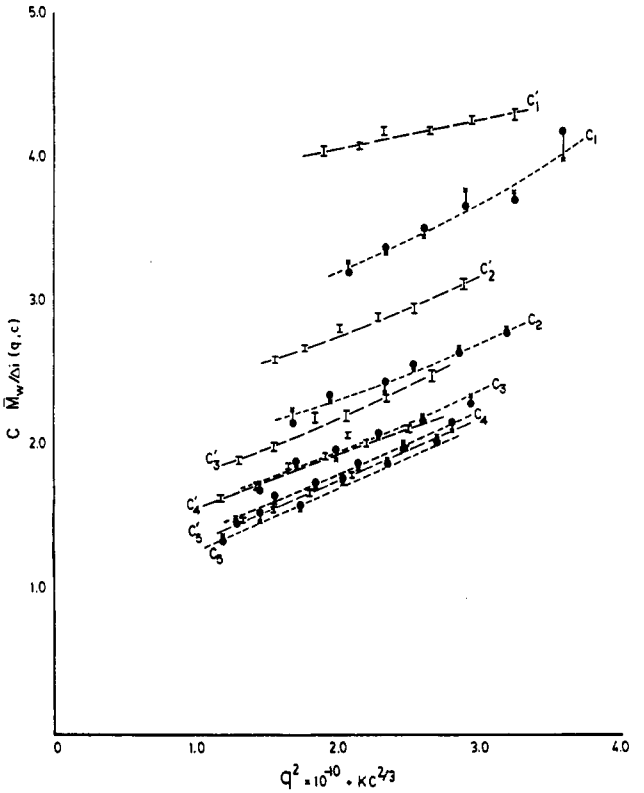

Figure 11. Plot of $cM_w[\Delta i(q,c)]$ against $q^2 \times 10^{-10} + Kc^{2/3}$ for $M_w = 3.84 \times 10^6$: (●) ethylbenzene, $C_1 = 1.07 \times 10^{-3}$ g/mL; (I) THF, $C' = 1.00 \times 10^{-3}$ g/mL and $C_{n+1} = C_n/2$, where $n = 1$–4.

that the local conformation is more flexible in THF.

It is interesting to speculate on the nature of the change in microstructure proposed on the basis of our studies. It has long been known that "atactic" polystyrenes exhibit a "conformational transition" at $T \approx 80$ °C from a low-temperature, comparatively rigid chain to a more flexible structure.[40] Application of a variety of spectroscopic methods suggests that this effect is due to thermal disruption of isotactic runs which exist, for $T < 80$ °C, in a 3_1 helical structure. It is possible that these conformers are stable in aromatic solvents like benzene, but are destabilized in THF. It is noted, in this connection, that the likely solvation mechanism of polystyrene by THF involves the formation of a weak charge-transfer interaction with the pendant phenyl rings.

RG theory envisions that the static and dynamic behaviors of long-wavelength concentration fluctuations ex-

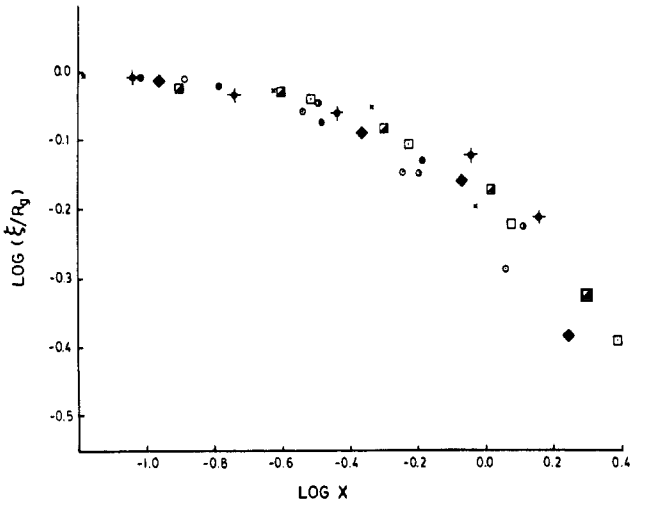

Figure 12. Universal plots after Wiltzius et al.,[41] log (ξ/R_g) against log x. In THF: (◑) 0.9×10^6; (*) 1.80×10^6; (♦) 3.84×10^6; (◪) 5.48×10^6. In ethylbenzene: (○) 1.8×10^6; (●) 3.84×10^6; (◆) 5.48×10^6; (□) 8.46×10^6.

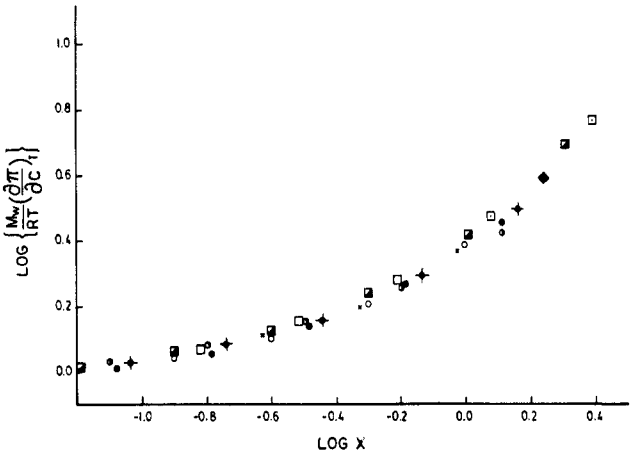

Figure 13. Universal plots after Wiltzius et al.,[41] log M_w/RT-$(\partial\pi/\partial c)_T$ against log x. Symbols same as in Figure 12.

hibit "universal" behavior for sufficiently high molecular weights; i.e., their properties are independent of the details of the microscopic structure and will show a smooth universal crossover to the semidilute regime. Wiltzius et al.[41] recently showed that the quantities (ξ/R_g) and $(M_w/RT)(\partial\pi/\partial c)_T$ defined by

$$\frac{Kc}{\Delta R_\theta} = \frac{1}{RT}\left(\frac{\partial\pi}{\partial c}\right)_T (1 + \xi^2 q^2 + O(q^4)) \qquad (32)$$

are universal functions of $x = (16/9)A_2M_wc$ for polystyrenes dissolved in two rather different solvents (toluene and methyl ethyl ketone). In Figures 12 and 13 we test the universalities of quantities (ξ/R_g) and $(M_w/RT) \times (\partial\pi/\partial c)$ with respect to x. Our experimental data, although limited in concentration and q vector range, superimposes quite well, conforming to the observations presented by Wiltzius et al.[41]

On the basis of these results, we anticipate that an appropriate scaling function $\bar{F}$ is of the form $\bar{F}(qR_g,x)$. This hypothesis is tested in Figure 14 which shows that the reduced quantity $D_q^{1/2} = [M_w(Kc/\Delta R_\theta)]^{1/2}$ exhibits universal scaling when plotted vs. $q^2R_g^2 + K'x$, as we have demonstrated previously in an earlier report.[42] We find that this scaling form works well for THF and ethylbenzene, the universal function $\bar{F}(q,c)$ having very similar empirical properties to that found by Wiltzius et al.[41] It is noted that recent progress has been made in theoretical

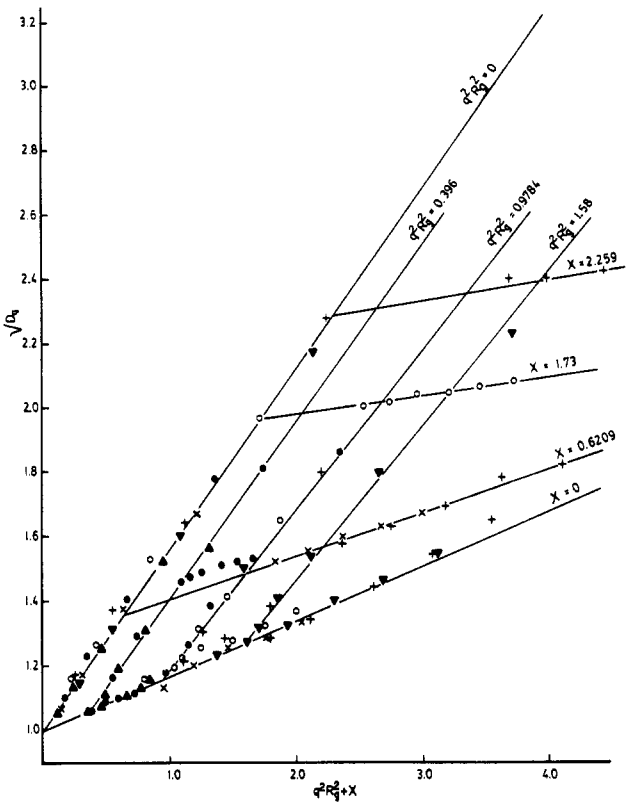

Figure 14. Universal plots of $[M_w(Kc/\Delta R_\theta)]^{1/2}$ against $q^2R_g^2 + K'x$ (K' is an arbitrary constant). In THF: (▲) 1.8×10^6; (○) 3.84×10^6; (▼) 5.48×10^6. In ethylbenzene: (•) 1.8×10^6; (x) 3.84×10^6; (+) 5.48×10^6. The experimental values at a finite x and $q^2R_g^2$ are chosen close to that specified in the plot.

understanding of the function $\bar{F}(qR_g,x)$.[43,44] However, quantitative estimates of the universal ratios, including the interpenetration parameter ψ, appear to be prone to comparatively large uncertainties.[44]

In summary, Table V together with Figure 11 clearly demonstrate that polystyrene behaves differently in THF than in ethylbenzene, benzene, or toluene in this molecular weight range. The possible consequences for theory and interpretation of experiment are significant. First, it is possible that in either THF or EtPh there is a breakdown of the fundamental Rayleigh–Gans–Debye (RGD) assumptions used in relating light scattering data to molecular structure. Such effects have been recently discussed theoretically[45] but do not appear to be relevant to our studies. For example, we obtain identical M_w values in each solvent. It is also noted that previous experimental tests of the validity of the RGD theory support its validity in molecular size and range and for polarizability contrast values pertinent to this work.[46] Next, it is possible that at these molecular weights THF is not in the asymptotic excluded-volume, asymptotic nondraining limit, but that ethylbenzene and its related solvents benzene and toluene are. This would, however, be rather extraordinary, as THF in this region appears to have a larger excluded-volume interaction (manifested in the larger A_2 or $(\partial\pi/\partial c)$ and to be less draining (on the basis of the hydrodynamic ratio U_{η_c}). Theory suggests that if the short distance scale (small polymer) excluded volume is small or the short distance scale draining is large, the crossover to the asymptotic range should be very slow; conversely, the crossover from large excluded volume and/or little draining to the near asymptotic region is relatively fast. Moreover, we expect these crossovers to be monotonic[7] or nearly monotonic.[13,14] Thus, the larger long distance excluded volume and smaller draining observed in THF suggests that if THF is not in

the asymptotic range, there is substantial doubt that the other solvents are. This would indicate that good comparison[9] of theoretical predictions of universal ratios with experimental results (as seen in the polystyrene–ethylbenzene system, for example) is accidental and both theory and experiment must be improved. Finally, it is also possible that these ratios are, in fact, not universal, as was once suggested by precise experiments on related systems.[47] However, more recent analysis has confirmed two-length scale universality for these data.[48] If two-length scale universality is to be valid for polystyrene in EtPh and in THF, it is necessary to propose both that THF is a better solvent than EtPh and that there is a change in microstructure in THF to a more flexible conformation.

Any one of the above possibilities are of considerable interest and mandate further study of identical, higher molecular weight polystyrenes in these solvent systems at low wavevectors over a wide range of concentrations. Our light scattering studies, as shown in Figure 14, are presently confined to a relatively small region of (q, c) space. Analyses of the dynamic structure factor of the polystyrene–benzene and polystyrene–toluene systems have been interpreted as being representative of the nondraining good-solvent limit. Our experiments suggest this deduction may be premature. Previous authors have noted[43,49,50] that even for comparatively homogeneous polymers like polystyrene the effects of polydispersity must be carefully evaluated in testing light scattering data vs. theoretical prediction. Our results indicate that for polystyrene one may also have to consider solvent-induced changes in microstructure when comparing solvents of comparable solvating power. Our present data suggest that the THF system is closer to the nondraining, good-solvent limit than the chemically-related systems benzene, toluene, and ethylbenzene.

Acknowledgment. We thank the National Science Foundation for support of this work through research awards CPE 80-17821 and DMR 81-19425.

Registry No. EtPh, 100-41-4; THF, 109-99-9; polystyrene (homopolymer), 9003-53-6.

References and Notes

(1) Zimm, B. *Macromolecules* **1980**, *13*, 592.
(2) Fixman, M. *Macromolecules* **1981**, *14*, 1706.
(3) Barrett, A. J. *Macromolecules* **1984**, *17*, 1566.
(4) Guttmann, C. M.; McCrackin, F. L.; Han, C. C. *Macromolecules* **1982**, *15*, 1205.
(5) Barrett, A. J. *Macromolecules* **1984**, *17*, 1551.
(6) de Gennes, P. G. "Scaling Concepts of Polymer Physics"; Cornell University Press: Ithaca, NY, 1979; Chapter 10, p 265.
(7) Barrett, A. J.; Domb, C. *Proc. R. Soc. London* **1981**, *376*, 366.
(8) Lax, M.; Barrett, A. J.; Domb, C. *J. Phys. A: Math. Gen.* **1978**, *11*, 361.
(9) Oono, Y.; Kohomoto, M. *J. Chem. Phys.* **1983**, *78*(1), 520.
(10) Shiwa, Y.; Kawasaki, K. *J. Phys. C.* **1982**, *15*, 5345.
(11) Douglas, J. F.; Freed, K. F. *Macromolecules* **1984**, *17*, 2344.
(12) Douglas, J. F.; Freed, K. F. *Macromolecules* **1984**, *17*, 2354.
(13) Weill, G.; des Cloizeaux, J. *J. Phys. (Les Ulis, Fr.)* **1979**, *40*, 99.
(14) Ackasu, A. Z.; Han, C. C. *Macromolecules* **1979**, *12*, 276.
(15) Miyaki, Y.; Einaga, Y.; Fujita, H. *Macromolecules* **1978**, *11*, 1180.
(16) Adam, M.; Delsanti, M. *Macromolecules* **1977**, *10*, 1229.
(17) Fukuda, M.; Fukutomi, F.; Kato, Y.; Hashimato, M. *J. Polym. Sci., Polym. Phys. Ed.* **1974**, *12*, 871.
(18) Appelt, B.; Meyerhoff, G. *Macromolecules* **1980**, *13*, 657.
(19) Utiyama, H.; Utsumi, S.; Tsunashima, Y.; Kurata, M. *Macromolecules* **1978**, *11*, 506.
(20) McDonnell, M. E.; Ramanathan, M. *Macromolecules* **1984**, *17*, 2093.
(21) McDonnell, M. E.; Jamieson, A. M. *J. Macro. Sci., Phys.* **1977**, *B13*, 67.
(22) Yu, T. L.; Reihanian, H.; Jamieson, A. M. *Macromolecules* **1980**, *13*, 1590.
(23) Neyerhoff, G.; Appelt, B. *Macromolecules* **1979**, *12*, 968.
(24) Schulz, G. V.; Baumann, H. *Makromol. Chem.* **1968**, *114*, 122.
(25) Spychaj, T.; Lath, D.; Berek, D. *Polymer* **1979**, *20*, 437.
(26) Lee, H.; Jamieson, A. M.; Simha, R. *Macromolecules* **1979**, *12*, 329.
(27) Zimm, B. H. *J. Chem. Phys.* **1948**, *16*, 1099.
(28) Berry, G. C. *J. Chem. Phys.* **1966**, *44*, 12, 4550.
(29) Jamieson, A. M.; McDonnell M. E. *Adv. Chem. Ser.* **1979**, *No. 174*.
(30) Stacey, C. J.; Kraus, G. *J. Polym. Sci., Polym. Phys. Ed.* **1979**, *17*, 2007.
(31) Tanford, C. "Physical Chemistry of Macromolecules"; Wiley: New York, 1961.
(32) Moraglio, G.; Matini, J. *Chim. Ind. (Milan)* **1965**, *47*, 744.
(33) McDonnell, M. E.; Jamieson, A. M. *J. Macromol. Sci., Phys.* **1977**, *B13*, 67.
(34) Yamakawa, H. "Modern Theory of Polymer Solutions"; Harper and Row: New York, 1971.
(35) Mandema, W.; Zeldenrust, H. *Polymer* **1977**, *18*, 835.
(36) Bawn, C. E. H.; Freeman, C.; Kamaladdin, A. *Trans. Faraday Soc.* **1950**, *4*, 1107.
(37) Jamieson, A. M.; Venkataswamy, K. *Polym. Bull.* **1984**, *12*, 275.
(38) Debye, P.; Bueche, A. M. *J. Chem. Phys.* **1948**, *16*, 573.
(39) Mijnlieff, P. F.; Wiegel, F. W. *J. Polym. Sci., Polym. Phys. Ed.* **1978**, *16*, 245.
(40) Reiss, C. *J. Chim. Phys. Phys.-Chim. Biol.* **1966**, *63*, 1299.
(41) Wiltzius, P.; Haller, H. R.; Cannell, D. S.; Schaefer, D. W.; *Phys. Rev. Lett.* **1983**, *51*, 1183.
(42) Venkataswamy, K.; Jamieson, A. M.; Petschek, R. G. *Polym. Commun.* **1985**, *26*, 101.
(43) Schafer, L. *Macromolecules* **1984**, *17*, 1357.
(44) Freed, K. *J. Chem. Phys.* **1983**, *79*, 6357.
(45) Dung, M. H.; Ladanyi, B. M. *Macromolecules* **1984**, *17*, 1238.
(46) Jennings, B. R.; Jerrard, H. G. *J. Colloid Sci.* **1965**, *20*, 448.
(47) Ahlers, G. "Quantum Liquids"; Rewalds, J.; Regge, T., Ed.; North-Holland: New York 1978.
(48) Singsaas, A.; Ahlers, G. *Phys. Rev. B: Condens. Matter* **1984**, *30*, 5103.
(49) Cotton, J. P. *J. Phys., Lett.* **1980**, *41*, 231.
(50) Douglas, J. F.; Freed, K. F. *Macromolecules* **1985**, in press.